Chapter 1

Power System Protection Design for NPP

Chang-Hsing Lee and Shi-Lin Chen

Additional information is available at the end of the chapter

http://dx.doi.org/10.5772/50557

1. Introduction

One of the key purposes of NPP power system protection is to ensure that NPP's local power demand (such as cooling pumps, control systems, etc.) are met under all circumstances even during faulted periods. To achieve this goal, NPP power system protection must ensure that it can supply these local loads using either (1) power from the grid (via the transmission connection, which in most time, however, are used for exporting the excess power generated by the NPP after supplying its local loads) or (2) power from local generations such as diesel generators, batteries, etc. at all times and under all circumstances.

On the first power source (grid power), many NPPs worldwide have been built along the seashore for cooling water availability reasons. Overhead transmission lines are thus built in the vicinity of the seashore to transport the large amount of power generated from the NPP to the grid economically. As these overhead lines are exposed to salt contamination, flashover will occur when contamination becomes excessive. In the event of flashover, which is equivalent to a line-to-ground fault, the plant's protection system will need to initiate a series of switching operation to redirect the large power output from the NPP to a backup route in order to avoid reactor emergency shut-down. However, such switching has the adverse effect of causing undesirable transient overvoltages to propagate in the plant's local power grid [1-4]. Dealing with the frequent switching actions of these overhead lines while mitigating their adverse effects thus becomes the first challenge of designing NPP power system protection.

Once the NPP loses its connection to the grid, it will need to rely on the local generation to continue supplying its local loads. Most NPP use multiple "independent" sources as backup power. However, unless NPP's local power grid is properly configured and its protection system properly designed, these "independent" sources can all fail at the same time as manifested in Taipower's 18 March, 2001 Level 2 event ("318 Event") [5].

In the following sections, we will examine Taipower's "318 Event" in detail to demonstrate the various possibilities that could lead to NPP plant blackout. Moreover, as these possibilities are not mutually exclusive, we will use this example to illustrate how multiple or cascaded problem can present further challenges to the overall NPP power system protection design. Recommended preventive measures are then summarized in the final section of this chapter.

2. Taipower "318 Event"

2.1. System configuration

Figure 1 shows the configuration of Taipower 3rd nuclear power plant. The NPP has two 951 MW generators which are connected to the local 345kV gas-insulated substation (GIS) in one-and-half breaker configuration as shown in Fig. 1. The NPP is then connected to the power grid via four 345 kV overhead power lines (Darpen 1, 2 and Lunchi Sea/Mountain) to the Darpen and Lunchi 345kV EHV (Extra High Voltage) substation and two 161kV overhead lines (Kengting and Fengkang) to Kenging and Fenkang 161kV HV (High Voltage) substation.

It is important to note that there are three 13.8 kV buses (in the middle) and four 4.16 kV buses (at the bottom) for plant utility. Among these buses, the two 4.16 kV buses in the middle are responsible for feeding the safety-critical equipment such as cooling pumps and are designated as “essential buses”. (The 2nd 4.16kV bus from the left where "DGA (Diesel Generator A)" is connected is designated as "Essential Bus A". The one next to it, where "DGB" is connected to, is "Essential Bus B".)

Another notable but subtle feature of this configuration is the use of 3-phase gas-insulated line (GIL) design with the 3 phases enclosed in a single duct of approximately 340 meters for the connection of the generation units and auxiliary systems, (located at the foot of a hill) to the 345kV GIS (on the top of the hill) due to topography feature of the location. This feature has implication on the generation and propagation of switching transients which will be explained in later sections.

2.2. Event sequence

On 18 March, 2001, a Level 2 event occurred at Taipower’s 3rd NPP, and the whole plant went into blackout from 00:45 to 02:58. The event started at 00:45 when EHV CB3510 (see Fig. 1, highlighted in red) was closed to energize the then-offline 345 kV/13.8 kV/4.16 kV start-up transformer (X01). Upon CB3510 closure, medium voltage (MV) CB#17 on "Essential Bus A" exploded damaging not only CB#17 but also CB#15. CB#15 formed a permanent ground fault keeping "Essential Bus A" at ground potential thus Essential Bus A became useless. CB #3 and #5 on "Essential Bus B" was then opened hoping DGB will start and supply power to those critical loads. However, DGB failed to start and the whole plant went into blackout. The only hope remained at that time was DG5 (on the far right in Fig. 1) which, however, needs to be started locally and manually. After 2 hour since the first problem occurred, DG5 was finally started and started to supply power to the critical loads via "Essential Bus B".

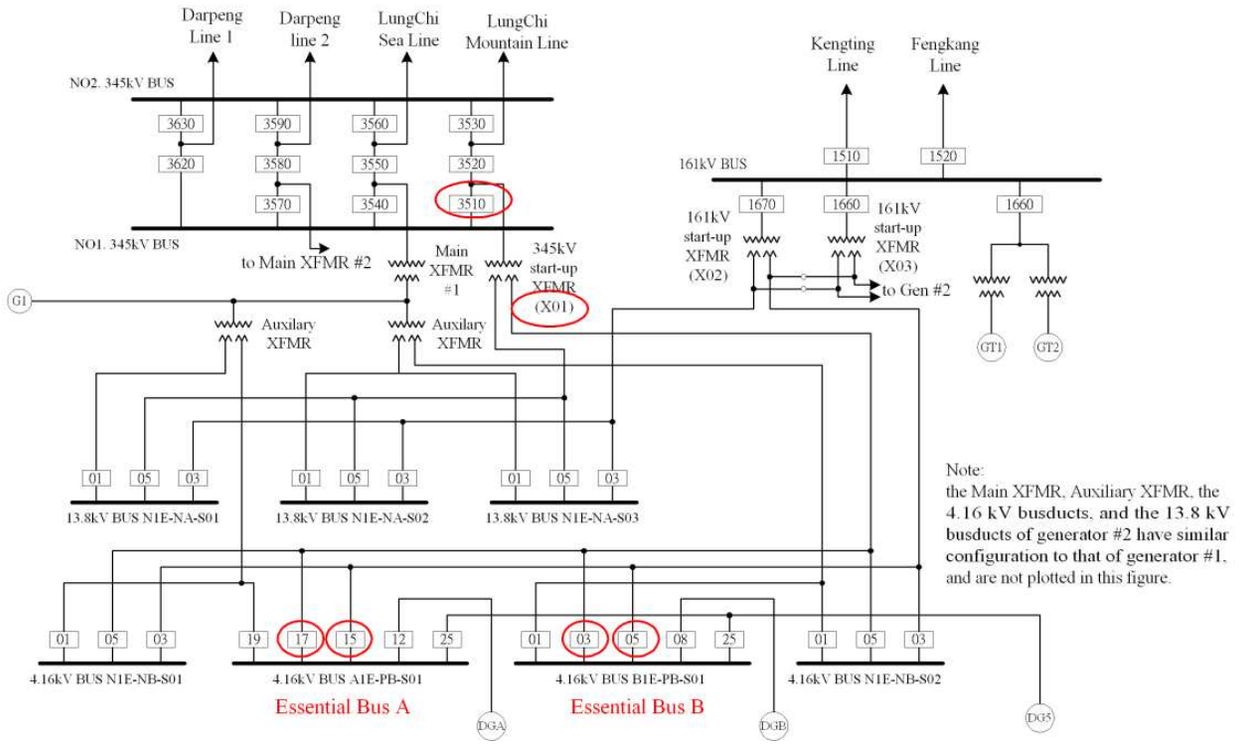

Figure 1. System Configuration of the NPP

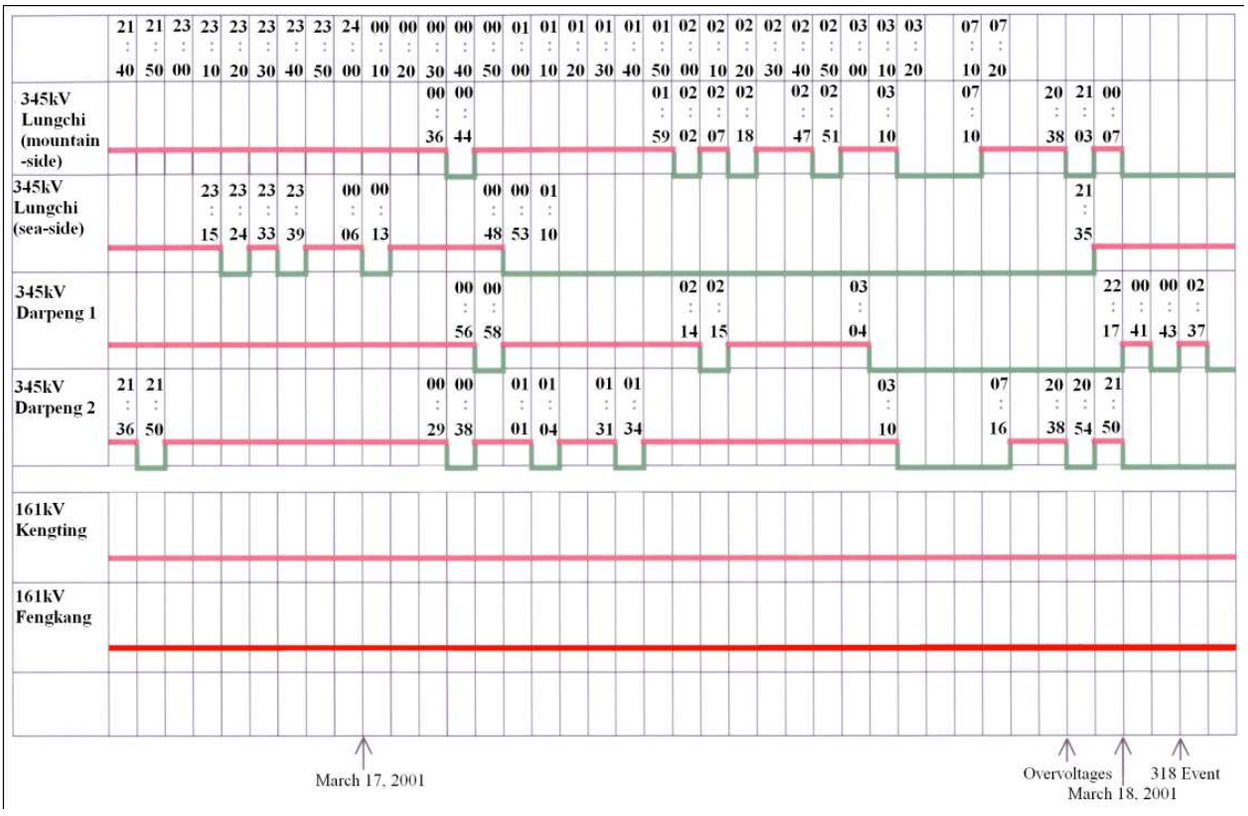

Figure 2. 345kV and 161kV Overhead Line Switching Event Log

Figure 2 shows the switching event log of the four 345kV and two 161kV lines connecting to the NPP. After reviewing the event log, it was found that CB#17 on Essential Bus A broke down when one GIS switching operation was occurring. The event log also showed that there were 37 EHV switching operations during the 48-hour period prior to the event due to salt-fog influence in the plant area. Because of the unstable offsite power, the GIS switched between different offsite power to acquire the stable power sources.

Figure 3 shows the transient recording of overvoltages for both the 345kV bus and one MV (medium voltage) bus at 20:38 in March, 2001. At t0, the flashover on the 345kV line occurred leading to its subsequent tripping at t1. The tripping took place on the remote end of the 345kV line thus overvoltage can still be observed at the NPP between t1 and t2 due to "motor-generating effects" to be explained in the following section of this Chapter. The overvoltage on the 345kV line eventually caused flashover from Phases A and B to ground pulling down the line voltage and all motors on the 4.16kV bus were tripped by their respective under voltage relays at t3. At t4, the flashover from Phases A and B to ground was cleared and the "motor-generating effects" start to build up the voltages again with the two remaining motors on the 13.8kV bus.

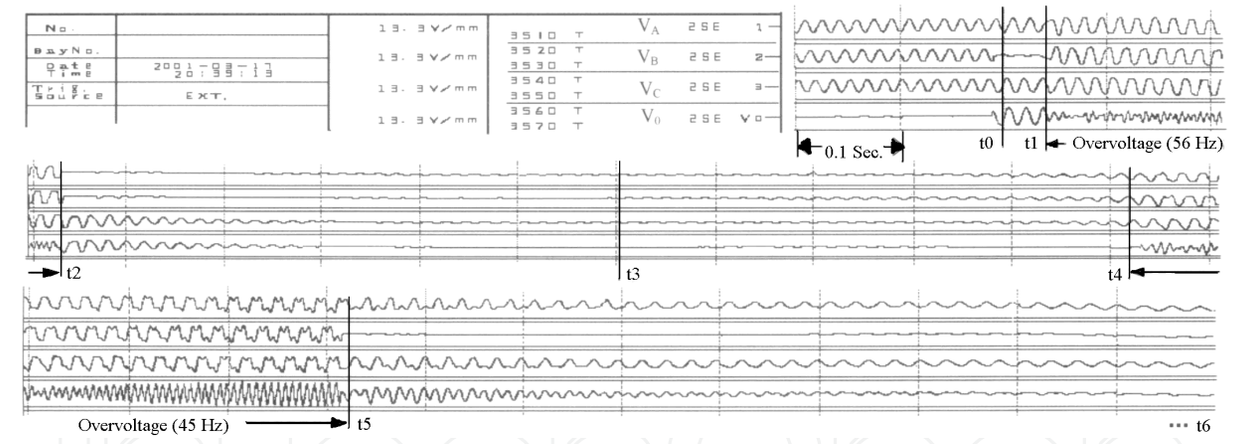

(a) Transient Recording at 345 kV GIS

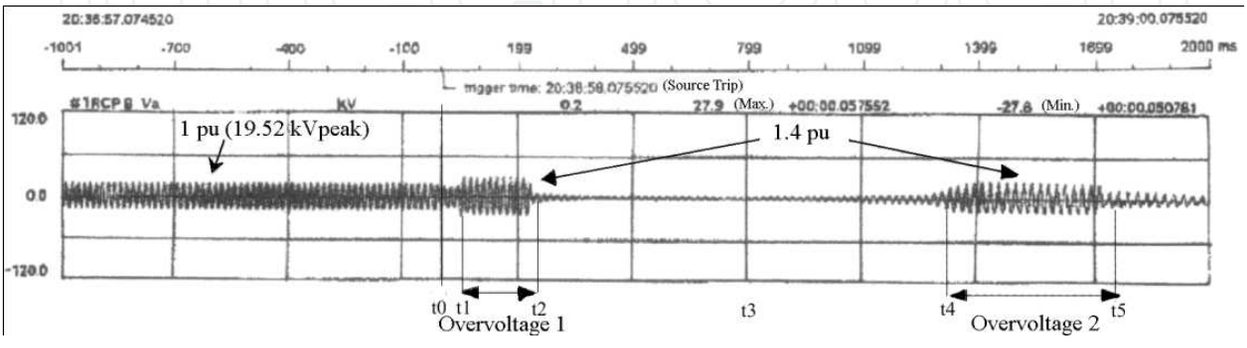

(b) Line-to-Line Voltage Transient Recording of one 13.8 kV motor, Recycle Colling Pump B

Figure 3. Overvoltages at 20:38 in March 17, 2001

2.3. Electrical stress in plant power system

2.3.1. Line conductor overvoltages due to over-excitation and nonlinear resonance [6,7]

The transient recorder in Fig. 3(a) recorded 2 abnormal overvoltages (at 56 Hz and 45 Hz, respectively) after the last 345 kV-transmission line connecting to the NPP was tripped on the remote end which turned the NPP into an electrical island. As will be explained in the next section, the 1st overvoltage was caused by the over-excitation of the motors (e.g. recycle water pump) in the plant who, with terminal voltages supported by large line capacitance, now operated as induction generator after loss of external power.

The 2nd overvoltage is caused by a different mechanism. After a few cycles the low voltage relays tripped many of the plant motors leaving only 2 biggest motor (now operating as induction generator) still connected and were supported by a comparatively much larger capacitance leading to not only over-excitation but also magnetic saturation of both the motors and transformers. This created a condition very close to ferroresonance resulting in even bigger overvoltage.

2.3.2. Neutral voltage transfer

It can be seen from Figure 3 that overvoltage were observed not only on the line conductors of phase A, B, and C but also on the neutral. As will be explained in the next section, neutral voltage transfer can occure through 2 different mechanisms: electromagnetic and capacitive transfer.

In the presence of transformer core saturation, 3rd harmonic neutral voltage will be present on the windings through electromagnetic transfer as long as the neutrals of the respective windings are not grounded. In the presence of neutral voltage on any of the transformer windings, the stray capacitance among the windings and earth will result in capacitive neutral voltage transfer.

2.3.3. Switching surges on both EHV and MV systems

From Fig. 2, it can be seen that there were 37 switching operations during the 48-hour period prior to the breakdown. This unusually high number of switching operation can create lots of switching surges (with magnitude of around 7 times the rated line-to-ground peak voltage in the medium voltage system) which, when propagating through the NPP local power network, can degrade the insulation level or even cause breakdown of CB's in the local power network [8,9].

It should be noted that while there were 37 switching operations on the EHV side, none of the switching surges were captured by the transient recorder in the 345kV GIS in Fig. 3(a) due to insufficient bandwidth of the transient recorder. In a follow-up field test [9] after the event, it was found that such switching often causes switching surges of around 7 times the rated line-to-ground peak voltage!

3. Stress mechanism and modeling

It can be seen from the above that Taipower's 3rd NPP was under sigificant and multiple stresses before and during the Level 2 event. This section explains the mechanisms working behind these stresses and provide basic principles how to model them.

3.1. Line conductor overvoltages due to over-excitation and nonlinear resonance [6,7]

Figure 3 shows that on Phases A, B, and C there were two overvoltages observed where the second overvoltage was slightly higher than the first. Causes of these 2 overvoltages are detailed as following.

3.1.1. First overvoltage (56Hz) – Over excitation

Figure 4 shows the 2 essential condition for induction motor generating effect: large capacitance and continuous rotating motor. When an induction motor lost its external voltage source, the flywheel with large inertia will keep the motor rotating and the capacitance of transmission line will provide the necessary voltage support for the induction motor to act as a generator. The magnitization curve of the motor and the amount of capacitance will jointly determine the overall motor generating effect as shown in Fig. 5. If the capacitance is too small to provide enough magnetizing current (curve C0 in Fig. 5), the terminal voltage of motor will decay exponentially and the generating effect will not sustain. However, if the capacitance is large enough, the motor generating effect will sustain and the terminal voltage is determined by the intersection of the capacitance and magnetizing curve such as (V1, C1) and (V2, C2) in Fig. 5.

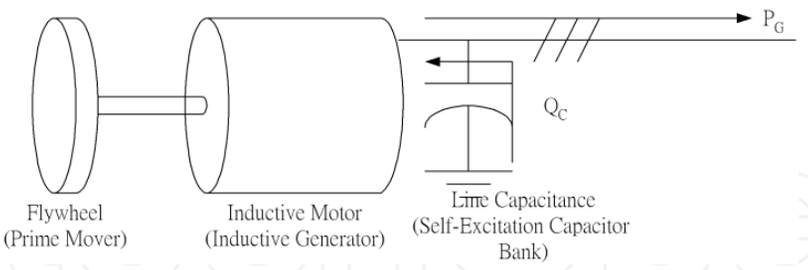

Figure 4. Equivalent Circuit of Motor-Generating Effect.

At "t1" in Fig. 3(a), the last 345kV transmission line connecting to the NPP was tripped on remote end due to a flashover on the line turning the NPP into an electrical island. As the local end of the 345kV line did not trip, a motor generating condition equivalent to Fig. 4 was formed with the 127kM transmission line providing sufficient capacitance to support the voltage of the various motors in the NPP. As can be seen in Fig. 3(b), the terminal voltage is increased to 1.4 p.u. and the overall resultant frequency is 56 Hz.

During this first overvoltage period, the terminal voltage of motor was about 1.4 p.u. (Fig. 3(b)) but the line voltage was about 1.29 times the rated line-to-ground peak voltage (Fig.

3(a)). This implied that the power transformers have saturated. As a result, a lot of harmonics were produced and the zero sequence components of them would be integrated into the neutral voltage resulting in unexpected high neutral voltage. This period ended at "t2" in Fig. 3(a) when the flashover grounded both phase A and B.

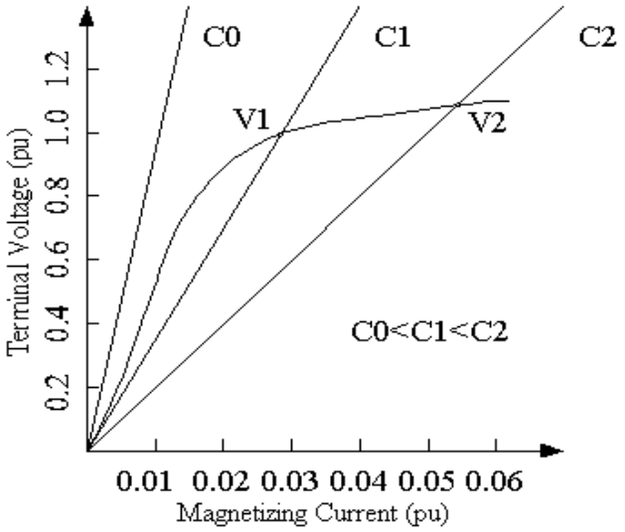

Figure 5. Relationships between Motor Terminal Voltage, Magnetization Curve, and External Capacitance

Table 1 shows the harmonic contents of B phase voltage between t1 and t2 in Fig. 3(a). The even order harmonics and DC component could be treated as the slight magnetic bias caused by asymmetric fault. At this stage, there was no ferromagnetic resonance in the island system.

Order	DC	1	2	3	4	5	6	7	8
%	9.3	100	7.8	8.0	3.6	13.5	1.6	6.1	1.2

Table 1. Voltage Harmonic Contents of Phase B between t1 and t2

3.1.2. Second overvoltage (45 Hz) - Nonlinear resonance

Figure 6 shows the four essential conditions for a ferroresonance to occur: voltage source, capacitance, nonlinear inductance (ferromagnetic and saturable), and low losses. The R in the RLC resonant circuit in Fig. 6 is very large due to the "low losses" condition and can often be ignored. The nonlinear inductance L is the magnetizing curve of the motors and transformers in the system and the capacitance is provided by the transmission line.

At "t3" in Fig. 3(a), all the motors on the 4.16 kV system were tripped by undervoltage relay. Between t3 and t4, the flashover grounding of phases A and B were cleared and the motor generating effects mentioned above picked up again gradually re-establishing the line voltage. At "t4" in Fig. 3(a), most motors in 13.8 kV system were also tripped by undervoltage relay with the exception of two largest ones. With the capacitance provided by the transmission line now need only to support the terminal voltage of 2 motors, we would

expect the terminal voltages to be higher than those during the first overvoltage stage according to Fig. 5. However, due to deep saturation of the motors and transformers, the overvoltage magnitude in Fig. 3(b) during the 2nd overvoltage is only slightly higher than the previous stage. This can be further seen from the fact that at the beginning of "t4" in Fig. 3(a), there were no overvoltage and no distortion of waveforms. As line voltage increased, the harmonics increased and after a few cycles the amplitude of voltage remained but voltage waveform distorted dramatically. Figure 7 shows the waveform at 4 cycle prior to t5 with its Fourier components summarized in Table 2 [10].

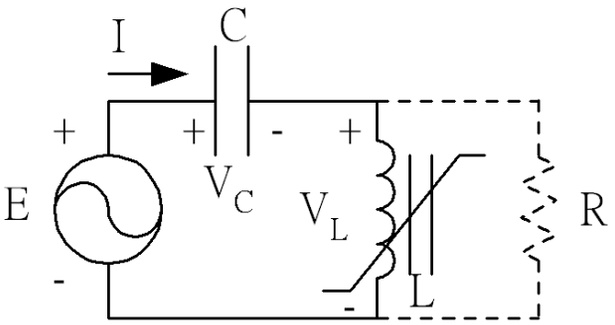

Figure 6. Equivalent RLC Circuit

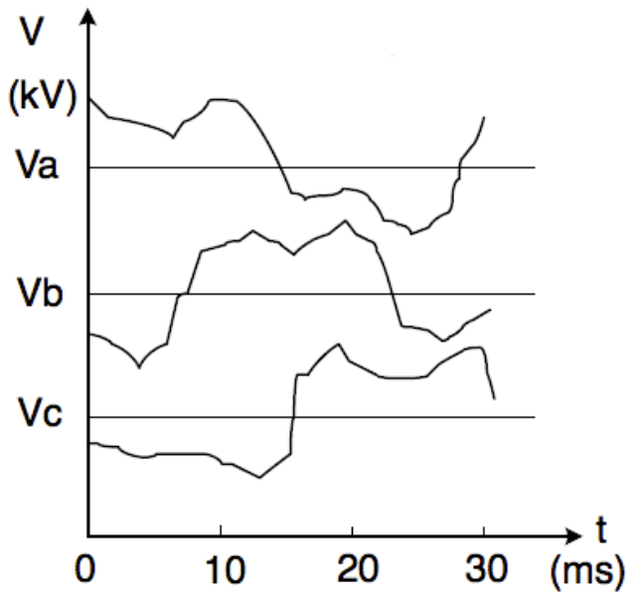

Figure 7. Zoom-in of The 4 Cycles prior to t5

It can be seen from Table 2 that the voltage of fundamental frequency was about 1.5 times the rated line-to-ground peak voltage, which is slightly larger than the previous overvoltage. The large DC and even-order harmonics indicate the deep saturation of the start-up transformer. In Table 2 the total of 3rd harmonics is 554.7 kV_{peak} (Note: The 3rd harmonics are in-phase therefore can be added up directly.) Comparing this figure with the neutral voltage of 626 kV_{peak} in Fig. 3(a), this indicates that 3rd harmonics is the main source of neutral voltage during the second overvoltage period.

order	Phase A		Phase B		Phase C	
	V_{peak}	%fund.	V_{peak}	%fund.	V_{peak}	%fund.
0	175.068	0.429	48.279	0.113	71.93	0.017
1	408.273	1.0	427.991	1.0	413.726	1.0
2	108.386	0.265	47.287	0.11	39.829	0.096
3	179.679	0.44	179.734	0.42	195.357	0.472
4	41.29	0.101	28.313	0.066	24.702	0.06
5	28.13	0.069	30.829	0.072	65.626	0.159
6	13.036	0.044	10.364	0.024	22.34	0.054
7	12.562	0.031	22.126	0.052	37.579	0.091
8	15.84	0.039	28.219	0.066	7.708	0.019
9	14.315	0.035	8.207	0.019	39.509	0.095
10	9.428	0.023	16.289	0.038	6.203	0.015
11	18.092	0.044	14.962	0.035	27.434	0.066
12	18.805	0.046	27.966	0.065	25.323	0.061
13	15.387	0.038	11.466	0.027	22.233	0.054
14	15.717	0.038	10.323	0.027	24.685	0.06
15	13.897	0.037	24.991	0.058	13.998	0.034
16	1.992	0	36.961	0.086	12.173	0.029

Table 2. Fourier Analysis of Fig. 7

As the inductances in the systems are now deeply saturated, there is a possibility that ferroresonance can occur. (Note: Ferroresonance is nonlinear resonances in power system where the voltage and current may change from normal steady state to another steady state with large harmonic distortion.) The phenomenon can be best understood from a circuit perspective using Figure 6 as example. In Fig. 6, the total equivalent impedance of the circuit is (jX_L - jX_C). When the inductance is saturated and current further increases, it will drive the inductor into deeper saturation where the inductor impedance jX_L will reduce when current further increases. A critical point will be reached at Point B in Figure 8 when (jX_L - jX_C) becomes zero. Any current increase beyond Point B will cause the total impedance change from a positive value to a negative value causing resonance effects near this operating point[7].

Based on analysis of all available data, it is believed that the 2nd overvoltage from t4 onward is on the boundary to be ferroresonance therefore the 2nd overvoltage is caused by a combination of motor-generating effect and nonlinear resonance.

3.2. Neutral voltage transfer [10]

It can be seen from Figure 3 that overvoltage can be observed not only on the line conductor but also on the neutral conductor as well. In order to understand this phenomenon we need to look at Fig. 9 where the equivalent circuit of a transformer is shown including its stray capacitances.

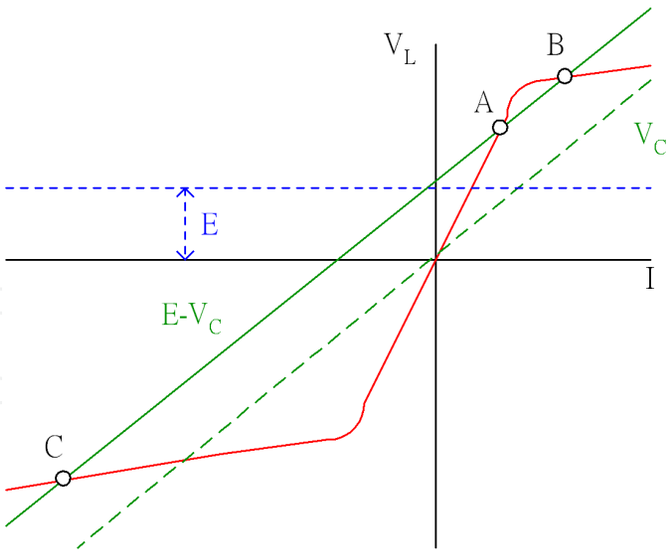

Figure 8. Ferroresonance Phenomenon Explanation

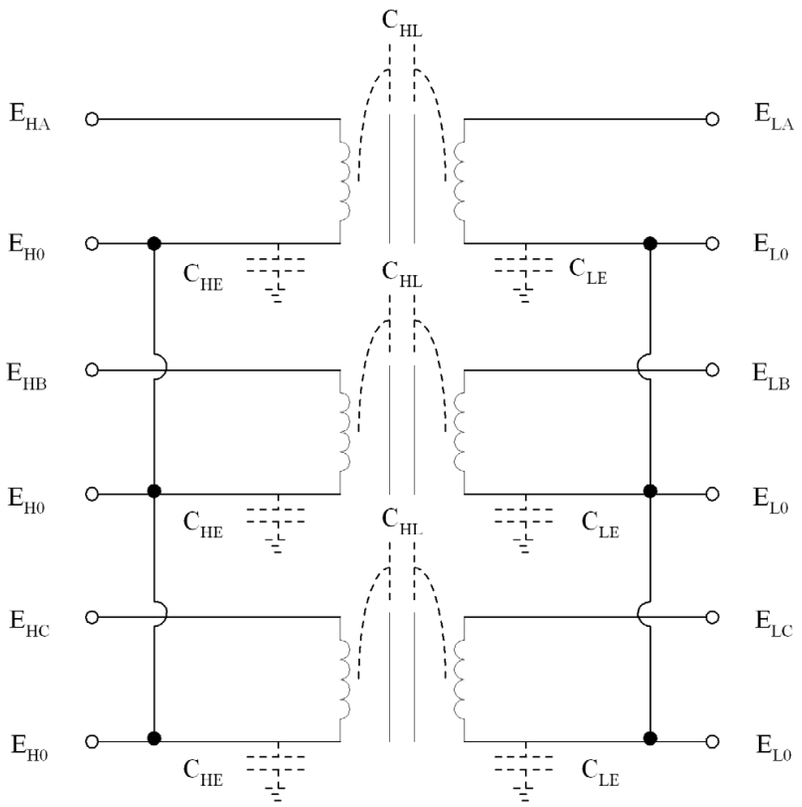

Figure 9. Voltage Transfer Diagram of 345 kV/4.16 kV Transformer

3.2.1. Transformer modeling

In Fig. 9, C_{HE} and C_{LE} depict the stray capacitance between high voltage (HV) winding to ground, and low voltage (LV) winding to ground, respectively, while C_{HL} depicts the stray capacitance between HV and LV windings. Typical stray capacitances for the 345/13.8/4.16kV power transformer are shown in Table 3.

In the presence of transformer core saturation, 3rd harmonic neutral voltage will be present on the windings through electromagnetic transfer as long as the neutrals of the respective windings are not grounded. Once the neutral voltage is established on any side of the neutrals, the stray capacitance provides a further path for it to transfer to other neutrals according to Equation (1)

$$E_{L0} / E_{H0} = C_{HL} / (C_{HL} + C_{LE}) \quad (1)$$

where E_{H0} is the neutral voltage at HV side, and E_{L0} is the neutral voltage at LV side.

Item	$C_{345/Earth}$	$C_{13.8/Earth}$	$C_{4.16/Earth}$	$C_{345/13.8}$	$C_{13.8/4.16}$	$C_{345/4.16}$
Capacitance	4.48 nF	13.76 nF	21.92 nF	4.3 nF	214.86 pF	8.96 nF

Table 3. Stray Capacitance of the 345kV/13.8kV/4.16kV Power Transformer

3.2.2. Neutral voltage transfer

It can be seen from Fig. 3(a) that, during 1st overvoltage the neutral voltage gradually roses to 200 kV_{rms} while during 2nd overvoltage the neutral voltage rose to 626 kV_{peak} (Note: the voltage waveform became very non-sinusoidal during 2nd overvoltage, we thus use peak value instead of rms value). The source of both overvoltages in the neutral was due to motor and transformer saturation resulting in 3rd harmonic voltages at the neutral however during the 2nd overvoltage the waveform is much more distorted with higher harmonic content.

As indicated by Fig. 3(a), the neutral on 345kV side does not appear to have been effective grounded possibly due to grounding failure. The result is that very high neutral voltage was established on the 345kV neutral and if the 4.16kV neutral was not grounded it will see a neutral voltage (through capacitive neutral transfer) of

$$200kVrms * \frac{8.96nF}{8.96nF + 21.92nF} = 58.03kVrms$$

$$626kVpeak * \frac{8.96nF}{8.96nF + 21.92nF} = 181.54kVpeak$$

during 1st and 2nd overvoltages, respectively. To better appreciate various grounding combination's effect on the neutral voltage transfer, 3 simulations were conducted assuming grounding conditions as per Table 4 and their results are summarized in Table 5.

Item	345kV side	13.8kV side	4.16kV side
Case 1	Ground (direct)	Ground (8 Ω)	Ground (2.4 Ω)
Case 2	Non-Ground	Non-Ground	Non-Ground
Case 3	Non-Ground	Ground (8 Ω)	Ground (2.4 Ω)

Table 4. Grounding Condition for Simulating Capacitive Transfer

Table 5 shows that as the neutral voltages transferred to the 4.16kV bus can be as high as 13 times the phase-to-ground peak voltage which can pose significant threat to CB#17 as well

as other CB's. However, if the neutral systems were properly configured, the risk can be minimized greatly.

	345kV side Phase Voltage	345kV side Neutral Voltage	4.16kV side Neutral Voltage
Case 1	457.55 kV_{peak}	0 kV_{peak}	0 kV_{peak}
Case 2	450.6 kV_{peak}	275.88 kV_{peak}	42.29 kV_{peak}
Case 3	448.93 kV_{peak}	44.58 kV_{peak}	0.002 kV_{peak}

(a) 1st overvoltage

	345kV side Phase Voltage	345kV side Neutral Voltage	4.16kV side Neutral Voltage
Case 1	428.83 kV_{peak}	0 kV_{peak}	0 kV_{peak}
Case 2	418.7 kV_{peak}	263.43 kV_{peak}	41.08 kV_{peak}
Case 3	420.94 kV_{peak}	46.25 kV_{peak}	0.002 kV_{peak}

(b) 2nd overvoltage

Table 5. Capacitive Transfer Simulation Result

3.3. Switching surges and Very Fast Transient Overvoltage (VFTO)

Switching operations are the most prominent phenomenon in the "318 Event". During the 48 hours prior to the Level 2 event, there were 37 switching operations and each could cause switching surges. Switching surges caused by GIS switching is characterized by its nanosecond wavefront and is commonly referred to as Very Fast Transient Overvoltage (VFTO) [11].

VFTO is the phenomenon of transient overvoltage generated during switching operation characterized by very short rise-time of 4 to 100 ns and has been covered by various literatures [3,12-22]. The phenomenon is particularly significant during Disconnect Switch (DS) operation due to multiple-restriking in the DS due to lack of arc-suppressing chamber.

3.3.1. Field measurement

In the past, VFTO was not considered to be possible to transfer from EHV through power transformer to medium voltage (MV) system [12-14]. However, in light of the "318 Event", a field test was conducted in Taipower 3rd NPP during plant overhaul by switching the DS of EHV GIS and measure the voltage on "Essential Bus A".

Field test result [9] shows that after switching the DS of EHV GIS, multiple 25 kV-level restrikes (approximately 7 times the rated line-to-ground peak voltage) were measured on the 4.16kV bus indicating VFTO can be transferred from the EHV side to MV side. It also indicates that the maximum peak voltages measured on the 4.16kV bus occur neither on the first strike nor on the last strike, and this behaviour is quite different with that in EHV system. The measurement results are shown in Fig. 10.

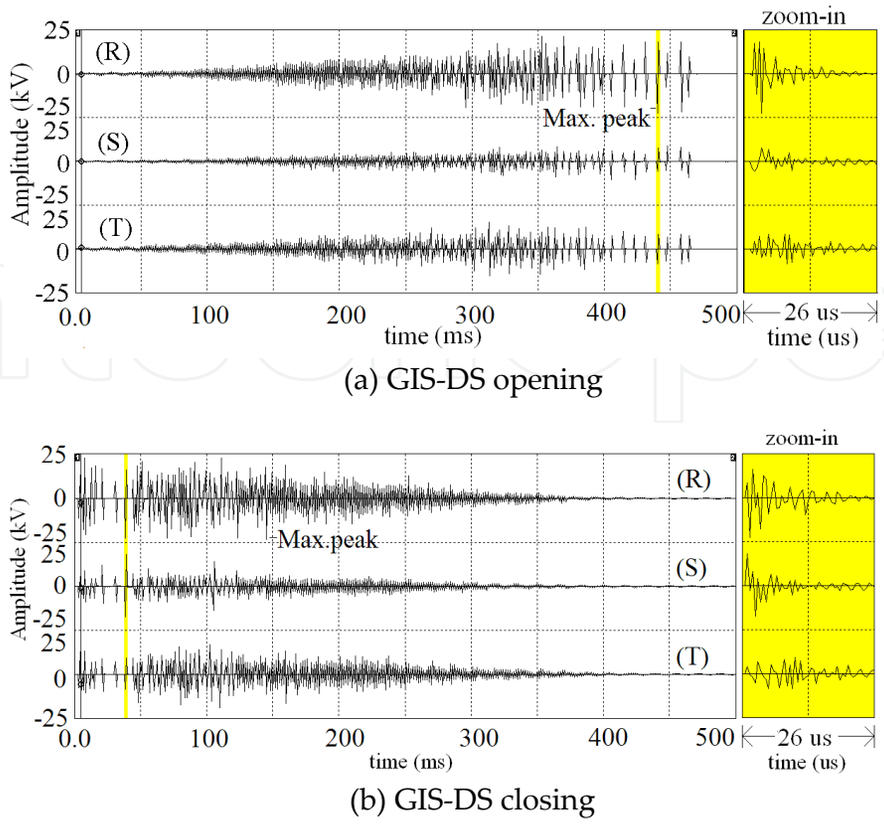

Figure 10. Switching Surge Measured on 4.16kV Bus by Operating EHV GIS Disconnect-Switch. (Note: The bandwidth of the measurement system was 2MS/s, the highest achievable in 2003)

3.3.2. VFTO simulation

To further appreciate VFTO transfer mechanism, numerical simulation model was built [23]. To validate this simulation model, the field test condition for Fig. 10 was reconstructed and the simulation result is shown in Fig. 11. It can be seen from Fig. 11 that the waveform envelope are consistent with measurement for both DS opening and closing and that the maximum VFTO on the essential bus occurred neither at first nor at last strike.

We then change the DS operation angle for each 5° intervals to simulate different closing/opening condition and Table 6 and 7 summarizes the maximum EHV inter-contact breakdown voltage vs. maximum MV VFTO. The following can be observed from Table 6 and 7:

1. The VFTO transferred to the essential bus A can be as high as 28.77 kV, which is about 8.47 times the rated line-to-ground peak voltage.
2. For all simulations, the restrike that causes the maximum VFTO on "Essential Bus A" does not necessarily coincide with the one that caused the max inter-contact breakdown voltage on EHV side.
3. Among the 36 simulations for DS opening, the simulation that produces the highest inter-contact breakdown voltage on EHV side is not the same as the one that produces

the maximum VFTO on "Essential Bus A". This is also true for DS closing. E.g., Case #28 (δ_{oper} = 135°) of DS opening produces the highest VFTO in MV system (28.77 kV) while it was Case #18 (δ_{oper}=85°) that produces the highest inter-contact breakdown voltage on EHV side (354.2 kV).

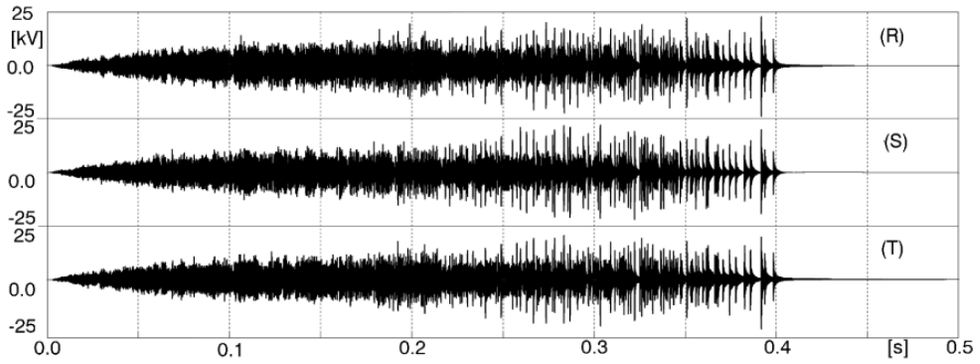

(a) GIS-DS opening

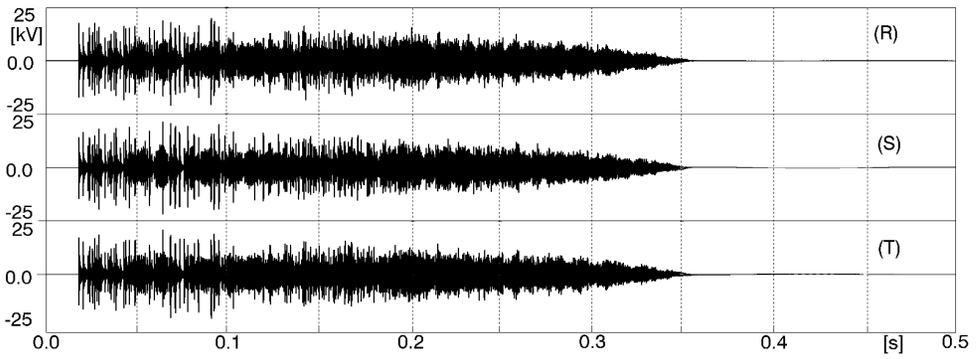

(b) GIS-DS closing

Figure 11. Simulation of VFTO at the Field Measurement Point

Item	Among the Multiple Restrikes				Total Num. of Restrikes on EHV Side per Φ
	Max. Inter-contact Breakdown Voltage		Max. VFTO at 4.16 kV		
	Mag. (kV)	Seq. Num.	Mag. (kV)	Seq. Num.	
Max. Inter-contact Breakdown Voltage Case # 18 among 36	354.2	467	23.76	444	468
Max. VFTO at 4.16 kV Bus Case #28 among 36	323.6	447	28.77	432	447

Table 6. Max. Inter-contact Breakdown Voltages vs. Max. VFTO in MV for DS Opening

Item	Among the Multiple Restrikes				Total Num. of Restrikes on EHV Side per Φ
	Max. Inter-contact Breakdown Voltage		Max. VFTO at 4.16 kV		
	Mag. (kV)	Seq. Num.	Mag. (kV)	Seq. Num.	
Max. Inter-contact Breakdown Voltage Case #14 among 36	284.8	1	23.27	12	460
Max. VFTO at 4.16 kV Bus Case # 23 among 36	278.0	1	26.41	26	455

Table 7. Max. Inter-contact Breakdown Voltages vs. Max. VFTO in MV for DS Closing

3.3.3. Characteristic of VFTO transferring to MV system

3.3.3.1. Capacitive coupling of high-turn-ratio transformer

VFTO and the oscillation voltages Vosc (voltages created by preceding restriking that can be superimposed to the following restrike) on the EHV side can be transferred to MV system through the start-up power transformer via capacitive coupling. The transfer ratio is mainly dependent on transformer's EHV-to-MV interwinding capacitance, transformer's MV winding-to-enclosure capacitance, and the bus-to-ground capacitance of MV system [23]. From both our measurement and simulation result, it was observed that the Vosc, which is of several tens kV in the EHV GIS, could still be of several kV in the MV system, and this will be superimposed to the VFTO coupled from the EHV side causing up to 7 ~ 8.47 times the rated line-to-ground peak voltage on MV side.

3.3.3.2. Superposition of oscillations initiated by a prior strike on top of subsequent restrikes

Figure 12(a) shows two consecutive restrikes from a multiple-restrike simulation and Fig. 12(b) shows its counterpart single-strike simulation. It can be seen from Fig. 12(a) that the Vosc initiated by the first restrike is superimposed to the second restrike resulting in a higher peak voltage (10.72 kV vs. the single strike one of 9.88kV).

3.3.3.3. Maximum VFTO transferred to MV for DS closing vs. DS opening

During DS opening the contact distance becomes wider and wider leading to longer intervals between two consecutive restrikes while that during DS closing is the opposite. As a result, there is a higher probability of superposition of Vosc to subsequent restrike during DS closing (thus higher VFTO) than opening.

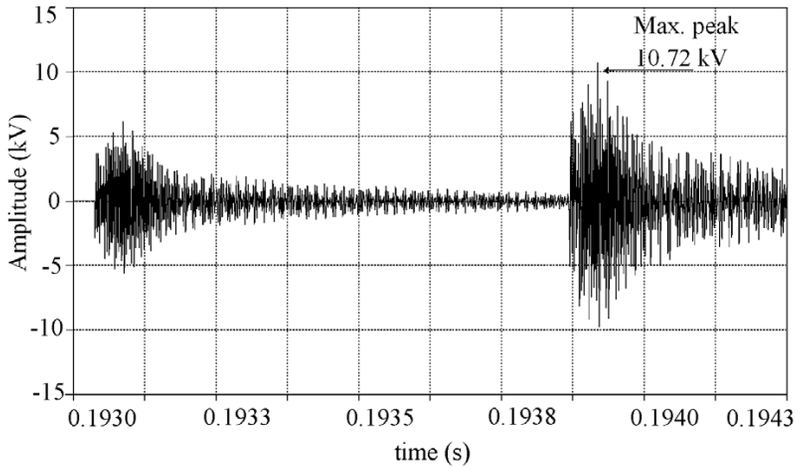

(a) Two consecutive restrikes taken out of multiple-restrike simulation of DS opening

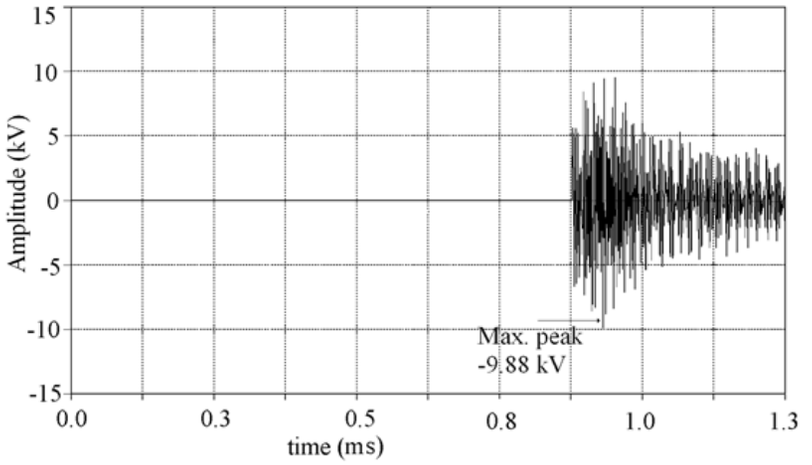

(b) Single-strike simulation with the same inter-contact breakdown voltage as in (a)

Figure 12. Oscillation Voltage (V_{OSC}) Initiated by a Strike or Restrike Can Be Superimposed to Subsequent Restrike Voltages.

4. Lesson learned and important aspects of NPP power system protection design

Events like the "318 Event" were seldom caused by one single reason. It can be seen from the above discussion that Taipower 3rd NPP was under multiple stresses before the event and there were mutiple mechanisms for the generation, amplification, and transfering of overvoltages which, combined with the operation practices and equipment history, eventually led to the explosion of CB#17 and total blackout of the NPP. Below are the key lessons learned from this event and their recommended preventive measure.

4.1. Bus configuration and fault area isolation

The "318 Event" was essentially triggered by a single equipment failure but leading to a complete blackout of the power plant. There are 2 key lessons learned from this event: (1)

Explosion of CB#17 took down the adjacent CB#15 as well. (2) "Independent sources" are not always independent due to improper bus configuration.

For various reason such as space requirement, ease of maintenance, etc, switchgear panels are usually installed in the same room side by side. If this cannot be changed, during the risk evaluation process one must consider the N-1 condition being loss of "one group of equipment" instead of "one equipment" unless sufficient separation are provided between the equipments.

The "independence" of power sources need then be examined closely. If multiple sources or multiple buses can be taken down by a single failure such as permenant fault to ground, etc, they cannot be considered as independent sources and more backup needs to be added.

It should be noted that during the "318 Event", after the explosion of CB#17 the plant utility room was filled with smoke which makes the manual starting of other diesel generators extremely difficult. Not only were equipments under significant stress but also the human operators. It is thus recommended that the feasiblity of starting backup sources under utility room smoke condition be checked and that any manual operation required during this stage be as simple and straightforward as possible with proper interlock to reduce the chance of human error which may further escalate the event.

4.2. Nonlinear resonance prevention

Among all the scenarios considered in this Chapter, nonlinear resonance is the most difficult one to be detected. In view of the potential hazard it could cause, precautionary measure must be taken to prevent it from initiating.

The first step is to prevent motor-generating effect from ever occuring (thus removing the key source of initiation.) As explained above, the essential conditions of motor-generating effect are (1) rotating motor with large inertia, (2) large capacitor bank in an isolation system to support the terminal voltage. Since a rotating motor with large inertia can not be stop immediately, the focus is to remove the capacitive support. In the case of Taipower 3rd NPP, the capacitive support came from the long transmission line who were tripped only on the remote end. It is recommended that Direct Transfer Trip (DTT) function be implemented for transmission line protection to greatly reduce the risk of motor generating effect.

The second step is to ensure effective grounding of transformer neutrals as designed. Due to the objective of minimizing short circuit current, the neutral groundings in NPP are usually multi-configured: arrestor grounded under normal condition and direct grounding when in islanding operation. The switching from one grounding scheme to another often requires manual operation and this increases the risks of leaving the islanded system ungrounded as well as nonlinear resonance of power. Proper interlock or checking mechanism should be implemented to ensure proper grounding as designed at all times.

4.3. Neutral voltage transfer

Neutral voltage transfer can occur via either electromagnetic or capacitive transfer. Based on simulation result the risk can be significantly reduced with proper grounding of the neutral. This, however, must be carefully implemented in order not to increase the short circuit current in the NPP.

Again, any manual operation during event would introduce extra risks therefore should be desigined to be as simple and straightforward as possible with proper interlock or checking system.

4.4. VFTO transferring to MV system

According to field measurement and numerical simulation, the VFTO transferring to MV system is usually underestimated by literatures. As demonstrated by both the field measurement and simulation result, peak voltage of VFTO in MV system could be as high as 8.47 times the rated line-to-ground peak voltage with an average 466 times restrike during DS operating [1,23]. Though the peak VFTO voltages transferred to the MV side are usually still within the basic impulse insulation level (BIL) tolerances of the equipment, this does not mean that repeatedly striking the equipment with 8.47 times the rated line-to-ground peak voltage would cause no damages to the equipment. In fact, this can accelerate equipment ageing and cause quick degradation of the insulation material and eventually leading to equipment breakdown.

After the "318 Event", a recommendation was made to Taipower No. 3 Nuclear Power Plant in 2003 for the installation of surge absorbers (0.8μF capacitor specially designed for surge absorption installed right close to the start-up transformer for each of the three phases) on the MV side in Fig. 1 [9,23]. The recommendation was adopted by Taipower in March 2005 and a subsequent measurement in March 2006 plus one-year monitoring indicated that there were no further VFTO exceeding rated line-to-ground peak voltage on the MV system.

4.5. Maintenance testing of in-service equipments

The damaged circuit breaker (CB#17) in Taipower 3rd NPP has been put into service for 20 years at the time of event. Maintenance testing history showed that insulation condition of this circuit breaker was good prior to the event however that being the case the circuit breaker should not have exploded when faced by transient voltage no higher than its BIL of 60kV. This shows that the current diagnostic method of insulation degradation (insulation resistance measurement, dielectric power factor measurement) may not be sensitive enough to detect insulation degradation due to ageing or repeated VFTO strikes. It is recommended that the reliability of such tests, including both the tool used, methodology employed, and interpretation of testing results (including monitoring the trend of measurement results) be further improved. For equipment subject to repeated switching surges, a higher standard should be applied.

5. Conclusion

Most NPP's in the world have been designed in such way that their local power loads are provided by "multiple independent sources" to ensure continuous power supply even during faulted periods. However, unless the NPP's local power grid is properly configured and its protection system properly designed, all these "multiple independent sources" can failed at same time as exemplified by Taipower's "318 Event". In view of the many similarities in design and other risk factors for world NPP's, it is of utmost importance that the lessons learned from Taipower's 3rd NPP "318 Event" be properly addressed.

This Chapter examines the Taipower "318 Event" in detail to demonstrate the various possibilities that could leads to NPP blackout. The possibilities investigated include: NPP's location factor, NPP local power grid configuration, cable parameters, switching events, switching surges propagating to MV circuits, ferroresonances, remote tripping, and manual starting difficulties. The lessons learned and proposed countermeasures are summarized in the previous section.

In summary, to ensure the proper design of NPP power protection system, the following 3 considerations must be incorporated:

1. **Check Independence of Equipment and Protection Zone for Various Scenarios:** The "318 Event" was caused by a single CB failure (CB#17) but leading to a complete NPP blackout for over 2 hours. This is mainly due to (1) the breakdown of CB#17 took down CB#15 at the same time due to their physical proximity. (2) The bus configuration cause none of the 2nd, 3rd, or 4th backup power to be available when both CB#15 and #17 both fails and CB#15 created a permanent line to ground fault. (3) The last resort (DG5) was located in a building filled with smoke caused by the CB#17's breakdown making manual starting extremely challenging. (4) The sustained overvoltage in the system could have been avoided should the tripping of the EHV cable be done on both ends of the line instead of just the remote end. All of the above suggest that the independence of equipment and protection zone have failed and needs to be taken into consideration when improving existing or future designs.
2. **Accumulated Equipment Stress Must be Monitored and Considered**: Particularly relevant for NPP's located on the seashore and subject to frequent line switching, equipment stress manifested in the form of reduced insulation level must be subject to more frequent and detailed monitoring. This would include not only absolute value measuring but also trending the measurement so that early signs of equipment weakness can be identified and proper measures be adopted to address it.
3. **Use System Protection Design Approach**: The cause of "motor generating effect", "neutral voltage transfer", "VFTO", and "ferroresonance" occurring during the "318 Event" cannot be addressed one by one and need to be taken into consideration from a system protection perspective. This would include the consideration for using different tripping scheme (such as Direct Transfer Trip on the EHV line) , adding additional protection device (such as installing surge absorbers on the MV bus), as well as reconfiguring the bus connections.

Abbrevious

BIL	Basic Impulse Level
CB	Circuit Breaker
DG	Diesel Generator
DS	Disconnect Switch
DTT	Direct Transfer Trip
EHV	Extra-High-Voltage
GIL	Gas-Insulated Line
GIS	Gas-Insulated Substation
HV	High Voltage
LV	Low Voltage
MV	Medium Voltage
NPP	Nuclear Power Plant
VFTO	Very Fast Transient Overvoltage

Author details

Chang-Hsing Lee
EE Dep. of National Tsing Hua University, Hsinchu, Taiwan

Shi-Lin Chen
EE Dep. of Chung Yuan Christian University, Chung Li, Taiwan

Acknowledgements

The authors wish to thank Professor He Zhao, Advisor to China Electric Power Research Institute, and Dr. Edward Hsi, EE Department, Chung Yuan Christian University, for their valuable comments on this work.

6. References

[1] Lee C. H., Hsu S. C., Hsi P. H., Chen S. L. Transferring of VFTO from EHV to MV System as Observed in Taiwan's No. 3 Nuclear Power Plant. in IEEE Trans. Power Delivery 2011, Vol. 26, No. 2: 1008-1016.

[2] Jakel W., Muller A. B. Switching Transient Levels Relevant to Medium Voltage Switchgear and Associated Instrumentation. in Proc. International Conference and Exhibition on ElectroMagnetic Compatibility, June 12-13, 1999.: 35-40.

[3] Buesch W., Marmonier J., Palmieri G., Chuniaud O., Miesch M. GIS Instrument Transformers: EMC Conformity Tests for a Reliable Operation in an Upgraded Substation. in Proc. Conference on Electric Power Supply Industry, Oct. 23-27, 2000.: 1-7.

[4] Uglesic I., Hutter S., Milardic V., Ivankovic I., and Filiovic-Grcic B. Electromagnetic Disturbances of the Secondary Circuits in Gas Insulated Substation due to Disconnector

Switching. in Proc. International Conference on Power Systems Transients, Sep. 28-Oct. 2, 2003.: 1-6
[5] Atomic Energy Council, The Station Blackout Incident of the Maanshan NPP unit 1: 2001.
[6] Tsao T. P., Ning C. C. Analysis of Ferroresonant Overvoltage at Maanshan Nuclear Power Station in Taiwan. IEEE Transaction on Power Delivery 2006, Vol. 21, No. 2.: 1006-1012.
[7] A. Greenwood, Electrical Transients in Power Systems. John Wiley & Sons, Inc.
[8] Das J. C. Surges transferred through transformers. in Proc. 2002 Annual Pulp and Paper Industry Technical Conference, 17-21 June, 2002.: 139-147
[9] Chen S. L. A study on The Feasibility to Install Surge Absorber at Low Voltage Side of 345 kV and 161 kV Start-up Transformer in The 3rd Nuclear Power Plant. Taiwan Power Company, Research Report, TPC-546-91-2104-10: 2003.
[10] Zhao H., personal communication: 2005.
[11] CIGRE WG 33/13-09 Very Fast Transient Phenomena Associated with Gas Insulated Substations, CIGRE Report: 1988.
[12] Meppeline J., Diederich K. J., Feser K., Pfaff W. R. Very fast transients in GIS. IEEE Trans. Power Delivery 1989, Vo. 4, No. 1.: 223-233.
[13] Fujimoto N., Boggs S. A. Characteristics of GIS Disconnector-Induced Short Risetime Transients Incident on Externally Connected Power System Components. IEEE Trans. Power Delivery 1988, Vol. 3.: 961-970.
[14] Kumar V. V., Thomas J. M., Naidu M. S. Influence of Switching Conditions on The VFTO Magnitudes in a GIS. IEEE Trans. Poer Delivery 2001, Vol. 16, No. 4.: 539-544.
[15] Popov M., Sluis L. van der, Smeets R. P. P., Roldan J. L. Analysis of Very Fast Transients in Layer-Type Transformer Windings. IEEE Trans. Power Delivery 2007, Vol. 22.: 238-247.
[16] Fujita S., Shibuya Y., Ishii M. Influence of VFT on Shell-Type Transformer. IEEE Trans. Power Delivery 2007, Vol. 22, No. 1.: 217-222.
[17] Shibuya Y., Fujita S., Tamaki E. Analysis of Very Fast Transients in Transformers. in Proc. IEE Generation, Transmission and Distribution Conference 2001, Vol. 148, Issue 5.: 377-383.
[18] Ogawa S., Haginomori E., Nishiwaki S., Yoshiida T, Terasaka K. Estimation of Restriking Transient Overvoltage on Disconnecting Switch for GIS. IEEE Trans. Power System 1986, Vol. 1, No. 2.: 95-102.
[19] Rao M. M., Thomas M. J., Singh D. P. Frequency Characteristics of Very Fast Transient Currents in a 245 kV GIS. IEEE Trans. Power Delivery 2005, Vol. 20, No. 4.: 2450-2457.
[20] Smeets R. P. P., Linden W. A. van der, Achterkamp M., Pamstra G. C., Meulemeester E. M. De Disconnector Switching in GIS: Three-Phase Testing and Phenomena. IEEE Trans. Power Delivery 2000, Vol. 15, No. 1.: 122-127.
[21] Christian J., Xie j. Very Fast Transient Oscillation Measurement at Three Gorges Left Bank Hydro Power Plant. in Proc. 2006 International Conference on Power System Technology, 22-26 Oct. 2006.: 1-7.

[22] Ji L. Y., Huang W. H., Zhang Z. Y., Shi W. Analysis and Simulation of Conducted Interference in Three-Phase in One tank GIS. in Proc. 2009 Second Asia-Pacific Conference on Computational Intelligence and Industrial Applications.: 269-299.
[23] Lee C. H. Simulation and Analysis of The Very Fast Transient Overvoltage in Medium Voltage Systems. Ph. D Thesis, National Tsing Hua University, Taiwan: 2011.

IntechOpen